Glycoconjugate Journal 20, 339–351, 2004

Transcriptional regulation of the human UDP-galactose:ceramide galactosyltransferase (hCGT) gene expression: Functional role of GC-box and CRE*

Tewin Tencomnao[1,2], Dmitri Kapitonov[3], Erhard Bieberich[1] and Robert K. Yu[1]

[1] *Institute of Molecular Medicine and Genetics, Medical College of Georgia, Augusta, GA 30912-2697, USA,* [2] *Department of Clinical Chemistry, Faculty of Allied Health Sciences, Chulalongkorn University, Bangkok 10330, Thailand,* [3] *Department of Neurosurgery, University of Pennsylvania, Philadelphia, PA 19104, USA*

UDP-galactose:ceramide galactosyltransferase (CGT, EC 2.4.1.45) is a key enzyme in the biosynthetic pathway of galactocerebroside (GalC), the most abundant glycolipid in myelin. Using a GalC expressing cell line, human oligodendroglioma (HOG), one which does not express GalC, human neuroblastoma (LAN-5), we previously demonstrated that the human CGT (hCGT) gene promoter functions in a cell-specific manner. Because the proximal (−292/−256) and distal (−747/−688) positive domains were shown to be critically involved in regulating the expression of several myelin-specific genes, we further investigated the functional roles of these two motifs in hCGT expression. Mutation analysis confirmed that a GC-box (−267/−259) and a CRE (−697/−690) were critical for hCGT expression. Electrophoretic mobility shift assay (EMSA) demonstrated that these motifs specifically bound to nuclear extracts from both cell lines. Using antibodies to Sp1, Sp3, pCREB-1, and ATF-1, these proteins were shown to be components of the EMSA complexes. However, the only difference between the HOG and LAN-5 cells was found in the EMSA profile of the CRE complexes. This difference may account for the differential transcription of the hCGT gene in the two cell types. Furthermore, the expression levels of ATF-1 detected were much higher in HOG cells than in LAN-5 cells. Thus, our data suggest that the GC-box and CRE function cooperatively, and that the CRE regulates the cell-specific expression of the hCGT gene.
Published in 2004.

Keywords: **translational regulation, transcription factors, galactocerebroside, UDP-galactose: ceramide galactosyltransferase**

Abbreviations: **ATF: activating transcription factors; bHLH: basic helix-loop-helix; bp: base pair(s); BSA: bovine serum albumin; bZIP: basic leucine zipper; CF1: common factor 1; CGT: UDP-galactose:ceramide galactosyltransferase; CRE: cAMP response element; CREB: cAMP response element-binding protein; ERE half-site, estrogen response element half-site; GalC: galactocerebroside; γ-IRE: interferon-γ response element; hCGT: human UDP-galactose:ceramide galactosyltransferase; HOG: human oligodendroglioma; kb: kilobase pair(s); LAN-5: human neuroblastoma; Luc: luciferase; MAG: myelin-associated glycoprotein; MBP: myelin basic protein; MOG: myelin-oligodendrocyte glycoprotein; MyT1: myelin transcription factor 1; NF-I-like: nuclear factor-I-like; NF-IL6: interleukin-6-regulated nuclear factor; P_0:protein zero; P_2:protein 2; PBS: phosphate-buffered saline; PLP: proteolipid protein; PMP-22: peripheral myelin protein-22; SCIP: suppressed-cAMP-inducible-protein; SGalC: galactosulfatide; TCF-1: T cell factor-1.**

Introduction

A crucial characteristic of the developing vertebrate nervous system is the ensheathment of axonal processes by myelin, a highly organized multilamellar structure formed by the plasma membranes of oligodendrocytes in the CNS and Schwann cells in the PNS [1]. The unique composition of myelin, with about 70% of the dry weight comprised of lipids, reflects its functional role as an electrical insulator that facilitates transmission of nerve impulses along the axon by saltatory conduction [1]. Galactocerebroside (GalC), from which sulfatide (SGalC) is derived, is the most abundant glycolipid in

To whom correspondence should be addressed: Dr. Robert K. Yu, Institute of Molecular Medicine and Genetics, Medical College of Georgia, 1120 15th Street, CA 1012, Augusta, GA 30912-2697, USA. Tel: 706-721-0699; Fax: 706-721-8727; E-mail: ryu@mail.mcg.edu
*This work was supported by an NIH grant, NS11853-30, to RKY.

myelin, constituting almost one-third of the myelin lipid [1–4]. Due to their abundance, and in conjunction with the results of numerous antibody perturbation studies, these galactolipids have been suggested to play a major role in the formation and maintenance of the myelin sheath [3,5–13]. GalC synthesis is catalyzed by the key enzyme UDP-galactose:ceramide galactosyltransferase (CGT, EC 2.4.1.45) [14–16], which transfers a galactosyl residue from UDP-galactose to ceramide. Our previous studies have also suggested that an augmented accumulation of GalC is likely mediated by an enhanced CGT activity [17,18]. Depending on whether 2-hydroxylated or non-hydroxylated ceramide is utilized as a substrate, two GalC isoforms are generated, suggesting their biosynthesis at different subcellular compartments [19].

The cloning of the CGT gene has provided powerful tools for further genetic analyses of galactolipid function [20–26]. The *cgt* locus spans approximately 70 kb and has been mapped to the distal region of human chromosome 4 band q26 [24] and to mouse chromosome 3 bands E3-F1 [25]. The CGT-deficient mouse models have been shown to highlight strikingly the importance of GalC in maintaining the functional integrity of myelin since these animals form unstable and dysfunctional myelin sheath [27–34], which has also been characterized by the loss of the rapid saltatory conduction velocity [31]. Little is currently known about the molecular regulatory mechanisms governing the hCGT gene expression. The expression of CGT gene is both developmentally regulated and tissue-specific corresponding to the myelination profile. In the rat CNS, a peak expression of CGT mRNA is observed at about postnatal day 20, concurrent with an active period of myelination [20–22]. The rat CGT transcript is brain-specific, expressed in similar regions as myelin basic protein (MBP), which correlates with white matter-containing structures [20]. Because the CGT gene expression is highly regulated and coordinated during myelination, the molecular regulatory mechanisms controlling both tissue-specific and developmentally regulated expression of this enzyme are of major interest. Understanding the regulation of hCGT gene expression might assist us in gaining insights into pathological conditions found in humans with demyelinating disorders such as multiple sclerosis and might eventually help in developing therapeutic approaches.

In the previous studies, we isolated and initially characterized the TATA-less hCGT gene promoter [35]. We also demonstrated that the hCGT promoter is highly active in human oligodendroglioma cells (HOG, $GalC^+$) but not in human neuroblastoma (LAN-5, $GalC^-$) cells, indicating that the hCGT promoter functions in a cell-specific manner [35]. This cell type-specific expression was also previously shown for the mouse CGT gene-promoter [36]. Three positive *cis*-acting regulatory domains were identified in the hCGT 5′-flanking region: (i) a proximal region located at −292/−256 which contains putative regulatory elements such as Ets and GC-box; (ii) a distal region localized at −747/−688 containing a number of transcriptional recognition sites such as estrogen response element (ERE) half-site, nuclear factor I (NF-I)-like, TGGCA, and cAMP response element (CRE); and (iii) a far distal region roughly mapped to −1325/−1083 consisting of several potential binding sites such as nitrogen regulatory site, T cell factor-1 (TCF-1), TGGCA, interleukin-6-regulated nuclear factor (NF-IL6), common factor 1 (CF1), basic helix-loop-helix (bHLH), NF-I-like, GATA, and interferon-γ response element (γ-IRE) [35]. However, we have never identified which transcription-factor binding sites located in these putative regulatory regions are truly involved in the hCGT transcription.

In the present studies, we focus on the GC-box (−267/−259) and CRE (−697/−690), two transcriptional elements previously identified in the proximal and distal positive regulatory domains of the hCGT gene since these have been shown to mediate the transcription of several myelin-specific genes [37]. More importantly, the high promoter activity appeared to be correlated with the presence of these two transcriptional elements in the hCGT 5′-flanking region, suggesting that GC-box and CRE are potential candidates for promoting the hCGT transcription [35]. Here, we employed EMSA and mutation analyses in order to investigate the significance of these two positive regulatory elements. Comparing the GC-box and CRE binding protein profiles of HOG cells, which express GalC, and LAN-5 cells, which do not, our findings suggest that the differential expression of hCGT may result from the differences between the nuclear proteins extracted from these two cell lines.

Materials and methods

Generation of hCGT promoter/luciferase reporter plasmid constructs

Following the PCR protocol using the 8-kb promoter region of hCGT cloned into pCR™ II plasmid as a template [26,35], we produced two plasmid constructs, phCGT(−826/−554)Luc and phCGT(−826/−554/−332)Luc, using two primers, −826F/*Sal*I and −554R/*Mlu*I tailed with a *Sal*I and an *Mlu*I site, respectively. All oligonucleotides used in this study are listed in Table 1. The former construct was made by cloning the PCR product directly into the promoterless luciferase expression vector, pGL3-basic vector (Promega); therefore, it did not contain the proximal regulatory region. The latter one was designed to contain the hCGT 5′-flanking fragment of −826/−554 cloned immediately upstream from the proximal promoter in phCGT(−332)Luc. This construct did not include the native intervening ∼220 bp between the proximal and distal regions. Instead, the two positive regulatory domains were separated from each other by less than 5 bp of the multi-cloning sites in the pGL3-basic vector.

Furthermore, we created reporter constructs containing a mutation in the putative control element (either GC box

Table 1. Oligonucleotide sequences and their locations used to generate promoter fragments of the hCGT gene

Name	*Oligonucleotide sequence*[a] *(5′ → 3′)*	*Position*[b, c]	*Construct*
−46R/*Nhe*I	caaaGCTAGCATCACTCGCCTCTGACTG	−46	
+40R/*Sma*I	caaaCCCGGGCGTGCGGCGAGCACAATC	+40	
−93F/*Sma*I	CAGCCCGGGGAGCTGGAGGCGCTC	−93	
−554R/*Mlu*I	ccg **ACGCGT**GCCTTAAAAAACGCGAGTTTGG	−554	
−826F/*Sac*I	caa*GAGCTC*CAATCTACCTCAGGCGCTC	−826	phCGT(−826/−554)Luc, phCGT(−826/−554/−332)Luc
GC mutagenic	GAAGAGTGGGAGGGGCCACGTG	−273	phCGT(mutated GC)Luc
Deleted GC	ccg **ACGCGT**GACACGCCTCGCAAAGAGGGA AGAGTΔCCACGTGCCGTTGTCAGAGTTCGC AACTCG	−292	phCGT(deleted GC)Luc
Deleted CRE	ccg **ACGCGT**TATGCTGCTGGCAAAGGCA GΔG ATAAAGTCGCCACAGGCTC	−717	phCGT(deleted CRE)Luc
−717F/*Mlu*I	ccg **ACGCGT**TATGCTGCTGGCAAAGG	−717	phCGT(−717)Luc

[a]Lower case denotes additional nucleotides flanking the restriction site for improving the cleavage close to the end of DNA fragments. The *Nhe*I, *Sma*I, *Mlu*I, and *Sac*I sites are indicated as underlined, double-underlined, bold, and italic letters, respectively. The specific mutated base is indicated as double-underlined. Δ represents a large deletion for the binding site of either GC-box (GGGCGGG) or CRE motif (ATTCGTCA).
[b]Nucleotide positions relative to the transcription start site (+1) of the hCGT gene.
[c]Except for −46R/*Nhe*I, +40R/*Sma*I, and −554R/*Mlu*I, the number designation in each primer corresponds to the DNA location of the first 5′ nucleotide of the oligonucleotide. F represents a forward primer (sense strand), and R indicates a reverse primer (antisense strand).

at −267/−259 or CRE at −697/−690) using different cloning strategies. Utilizing the transformer site-directed mutagenesis kit (Clontech), phCGT(mutated GC)Luc was generated by introducing a specific base change (C→A) into phCGT(−332)Luc following the manufacturer's instructions. Briefly, two mutant oligonucleotide primers were simultaneously annealed to one strand of a denatured double-stranded plasmid template, phCGT(−332)Luc. One primer referred to as the GC mutagenic primer was used to introduce the desired mutation. The second primer (the selection primer: GAGCTCTTGCGCGCGCTAGC) targeting outside the hCGT fragment was used to change the original unique restriction site (*Mlu*I: ACGCGT) into another unique restriction site (*BssH*II: GCGCGC) as indicated by underlined bases. For constructs containing a large deletion such as phCGT (deleted GC)Luc and phCGT(deleted CRE)Luc, the specific recognition site was deleted using the PCR approach primed with a long oligonucleotide primer without either GC-box or CRE in the middle of the sequence (Table 1) as described previously [38]. Since the 3′ ends of reporter plasmid constructs generated previously were terminated at 46 nucleotides upstream from the transcription start site [35], we extended the 3′ ends of these reporter constructs to +40 by inserting the 133-bp PCR fragment of hCGT 5′-flanking region, amplified using −93F/*Sma*I and +40R/*Sma*I primers, into the *Sma*I sites of the original reporter plasmid constructs. The integrity and orientation of all constructs were confirmed by restriction mapping and DNA sequencing.

Cell culture

HOG cells (a generous gift from Dr. Glyn Dawson, University of Chicago, Chicago, IL) and LAN-5 cells (a generous gift from Dr. Stephan Ladisch, Children's National Medical Center, Washington, D.C.) were cultured in Dulbecco's modified Eagle's medium and Roswell Park Memorial Institute 1640 medium, respectively, supplemented with 10% fetal bovine serum. Cells were maintained at 37°C in a humidified atmosphere at 5% CO_2.

Transient transfection assay

Transient transfections were performed using LipofectAMINE (Gibco) following the manufacturer's instructions. Briefly, HOG cells at about 70% confluence (approximately 5×10^5 cells) in a six-well plate were co-transfected with 2 μg of each reporter construct and 0.2 μg of the pHook^{TM} −2 *lacZ* vector (Invitrogen), which constitutively expresses β-galactosidase under the control of the CMV promoter, to monitor the transfection efficiency. In each transfection experiment, untransfected cells were included as controls for background levels of luciferase and β-galactosidase activities, and cells transfected with 2 μg of pGL3-basic were used as negative controls. Forty-eight hours after transfection, cells were lysed in 200 μl of the lysis buffer (Tropix). The luciferase activities in the cell lysates were determined using a Luciferase Assay System (Promega) and normalized to β-galactosidase activities determined using a Luminescent β-galactosidase Detection Kit

II (Clontech). Each reporter assay was performed using 20 μl of lysate in a ninety six-well plate and read using a microplate luminometer TR717/Winglow (Tropix). The data represent the mean ± S.D. of three independent experiments. Triplicate transfections were performed in each experiment. Luciferase levels were reported as fold elevation in activity over that seen in transfections with the promoterless pGL3-basic vector.

Preparation of nuclear protein extracts

Nuclear extracts from HOG and LAN-5 cells were prepared as described previously [39] with minor modifications. Briefly, cultured cells (5×10^7 to 1×10^8) were placed on ice, the medium was removed, and cells washed twice with ice-cold phosphate-buffered saline (PBS). Cells were manually scraped from the plates in 10 ml of PBS and collected by centrifugation at 250 × g for 10 min at 4°C. The cell pellet was resuspended in 2.5 ml of cell lysis buffer (buffer A; 10 mM HEPES, pH 7.9, 1.5 mM $MgCl_2$, 10 mM KCl, 0.5 mM dithiothreitol, 0.5 mM phenylmethylsulfonyl floride, 1 μg/ml aprotinin, 1 μg/ml pepstatin A, and 1 μg/ml leupeptin), allowed to swell on ice for 10 min, and then centrifuged at 250 × g for 10 min at 4°C. After the cell pellet was resuspended in 1.5 ml of cell lysis buffer, Nonidet P-40 was added to 0.05% and cells were homogenized with about 10 strokes of a tight-fitting Dounce homogenizer to release the nuclei. After the nuclei were collected by centrifugation at 250 × g for 10 min at 4°C, they were resuspended in 1 ml of nuclear extraction buffer (buffer C; 5 mM HEPES, pH 7.9, 26% glycerol, 1.5 mM $MgCl_2$, 0.2 mM EDTA, 0.5 mM dithiothreitol, 0.5 mM phenylmethylsulfonyl floride, 1 μg/ml aprotinin, 1 μg/ml pepstatin A, and 1 μg/ml leupeptin). The total volume was measured, and NaCl was added to a final concentration of 300 mM. The nuclear suspension was stirred on ice for 30 min, and then centrifuged at 24,000 × g for 20 min at 4°C. The supernatant was aliquoted, snap-frozen in dry ice/ethanol, and stored at −70°C before use.

Protein quantification

Protein concentrations were determined according to the Bradford method [40] using a protein assay kit (Bio-Rad) and bovine serum albumin (BSA) as the standard.

Electrophoretic mobility shift assay (EMSA)

EMSA was performed as described previously [39] with some modifications. The single-stranded oligonucleotides corresponding to the wild-type or mutant sequence of either GC-box (−267/−259) or CRE motif (−697/−670) were synthesized and annealed to generate double-stranded oligonucleotides with overhanging sequences. A stretch of five T residues at the 5′ end of the reverse oligonucleotide was added to increase the labeling efficiency. As shown below, the binding sequence for the corresponding transcription factor is designated in bold, and nucleotides carrying specific base changes (mutated nucleotides) for competition experiments are underlined.

Native GC-box: 5′- GAA GAG **TGG GCG GGG** CCA -3′
3′- CTT CTC **ACC CGC CCC** GGT TTTTT -5′

Mutated GC-box: 5′- GAA GAG **TG<u>T</u> <u>T</u>CG GGG** CCA -3′
3′- CTT CTC **AC<u>A</u> <u>A</u>GC CCC** GGT TTTTT -5′

Consensus GC-box (Promega): 5′- ATT CGA TC**G GGG CGG GG**C GAG C -3′
3′- TAA GCT AG**C CCC GCC CC**G CTC G -5′

Native CRE: 5′- TGG CAA AGG CAG **ATT CGT CA**G -3′
3′- ACC GTT TCC GTC **TAA GCA GT**C TTTTT -5′

Mutated CRE: 5′- TGG CAA AGG CAG **ATT <u>AT</u>T CA**G -3′
3′- ACC GTT TCC GTC **TAA <u>TA</u>A GT**C TTTTT -5′

Consensus CRE (Promega): 5′- AGA GAT TGC C**TG ACG TCA** GAG AGC TAG -3′
3′- TCT CTA ACG G**AC TGC AGT** CTC TCG ATC -5′

Approximately 10 pmol of each double-stranded oligonucleotide was labeled using filling-in reaction at the 3′-end with exo(−) Klenow polymerase (Stratagene) and [α-^{32}P]dATP. Labeled double-stranded oligonucleotide probes were purified by passage through a Sephadex G-50 column, then diluted using STE buffer (100 mM Tris-HCl, pH 8.0, 1 M NaCl, 10 mM EDTA) to a final concentration of 0.1 pmol/μl.

Typically, the nuclear protein-DNA binding reaction was performed for 20 min at room temperature in a total volume of 30 μl by mixing the binding solution (20 mM HEPES, pH 7.9, 1 mM MgCl, 0.5 mM dithiothreitol, 0.5 mM EDTA, and 4% Ficoll) with KCl to a final concentration of 50 mM, 2 μg of poly (dI-dC).poly (dI-dC), 1 μg of salmon sperm DNA, 100 fmol radiolabeled probe, and 2.5–10 μg of nuclear extracts. In competition experiments, a 50-fold excess of either unlabeled doubled-stranded wild type or mutant DNA probes was added to the reaction. In antibody supershift reactions, one of these polyclonal antibodies directed against Sp1 (sc-59×, Santa Cruz Biotechnology), Sp3 (sc-644×, Santa Cruz Biotechnology), or pCREB-1 (Ser^{133}, cat. #06-504, Upstate Biotechnology) was added to nuclear extracts and pre-incubated for about 10 min at room temperature before the addition of radiolabeled probe. The Santa Cruz Biotechnology's monoclonal antibodies directed against CREB-1 (sc-240×) and ATF-1 (C41–5.1×) were also utilized in supershift reactions using a native CRE as a probe. Protein-DNA complexes were separated on 5% non-denaturing polyacrylamide gel in 0.25× Tris-borate EDTA buffer at 180 V and 4°C, fixed, dried, and subjected to autoradiography for at least overnight at −70°C with an intensifying screen. Quantitation of DNA-protein complexes was performed using FluorChem™ Imaging System (Software 2.0, Alpha Innotech Corporation).

Western blot analysis

Briefly, twenty-five μg of nuclear extracts were fractionated by 15% SDS-polyacrylamide electrophoresis and electrotransferred to a nitrocellulose membrane (Bio-Rad). Transfer was confirmed by staining the blot with Ponceau S solution before proceeding with the antibody reaction. The membrane was incubated in blocking solution (4% nonfat dry milk, 0.1% Tween 20 in PBS or 3% BSA, 0.5% Tween 20 in PBS) for either 1 h at room temperature or overnight at 4°C. The blot was washed twice for 15 min each in PBS-Tween 20 (0.1%), then incubated overnight at 4°C with primary polyclonal antibody solution (2 μg of antibody/ml in 0.1% Tween 20, 5% BSA in PBS). The primary antibodies used were polyclonal goat anti-Sp1 (sc-59, Santa Cruz Biotechnology), polyclonal rabbit anti-Sp3 (sc-644, Santa Cruz Biotechnology), polyclonal rabbit anti-CREB-1 (cat. #06-504, Upstate Biotechnology), polyclonal rabbit anti-pCREB-1 (Ser^{133}, cat. #9191S, Cell Signaling Technology), and monoclonal mouse anti-activating transcription factor (ATF)-1 (C41-5.1, Santa Cruz Biotechnology). The blot was washed twice for 15 min each in PBS-Tween 20 (0.1%), then incubated for 1 h at room temperature with either a 1:5,000 dilution of the polyclonal donkey anti-mouse IgG coupled to horseradish peroxidase (Jackson ImmunoResearch), a 1:2,500 dilution of the polyclonal goat anti-rabbit IgG coupled to horseradish peroxidase (Sigma) or a 1:2,500 dilution of the polyclonal goat anti-mouse IgA coupled to horseradish peroxidase (Zymed Laboratories). After washing, the immunoreactive protein bands were detected using ECL Western blot detection system (Amersham Pharmacia Biotech).

Results

Characterization of the functional hCGT gene promoter

In this study, we analyzed the functional relationship between the proximal and distal regulatory sequences of the hCGT gene using two additional mutant reporter constructs. To determine whether the distal regulatory fragment is functionally dependent on the proximal promoter region, we generated the phCGT(−826/−554)Luc construct containing only the distal 5′-flanking region, from −826 to −554. Luciferase expression gained from HOG cells transfected with phCGT(−826)Luc construct, containing both distal and proximal regulatory fragments, was about 33-fold greater than that of the promoterless pGL3-basic vector; whereas, the distal region by itself evaluated in HOG cells transfected with phCGT(−826/−554)Luc was nonfunctional (Figure 1). To determine if the ∼220 bp spacer (from −553 to −333) located between the distal and proximal regulatory regions is crucial for the combined transactivation potential, we synthesized the construct, phCGT(−826/−554/−332)Luc that contained both distal and proximal *cis*-regulatory regions but not the intervening ∼220 bp. As shown in Figure 1, the transcription activity gained from

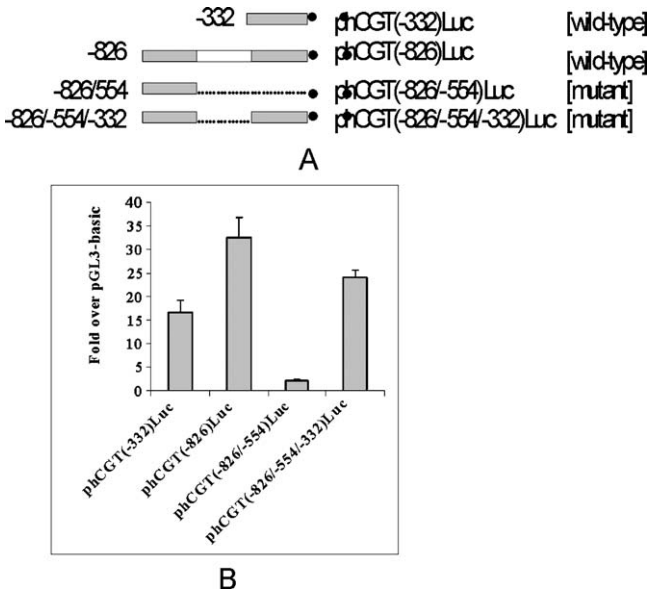

Figure 1. Functional relationship between the proximal and distal promoter regions. (A) A schematic representation of the constructs that contain the positive regulatory region(s) of hCGT gene inserted upstream of the luciferase coding region (indicated as a black arrow) in the pGL3-basic vector (Promega). phCGT(−826/554)Luc contains only the distal *cis*-region, but phCGT(−826/554/−332)Luc contains both distal and proximal positive *cis*-regions without the ∼220 bp spacer between them. The numbers in relation to the transcription start site (+1) indicate the position of the 5′ ends of the hCGT promoter/luciferase reporter constructs. Location of the positive regulatory regions is indicated by a gray box, whereas location of the deleted sequence is represented by a dotted line. (B) Functional activity of the promoter constructs in HOG cells. Each construct was co-transfected into the cells with pHook™-2 *lacZ* (Invitrogen). The luciferase activities of each deletion construct were normalized to the β-galactosidase activities. Activities are expressed as fold induction over pGL3-basic vector. Each value represents the mean ± S.D. of at least three independent sets of transfection experiments. Each set was performed in triplicate.

this construct was significantly diminished ($P < 0.05$), suggesting that this ∼220 bp spacer is crucial for transactivation.

Mutation analysis of putative *cis*-acting transcriptional elements

The presence of proximal (−292/−256) and distal (−747/−688) positive regulatory domains in the hCGT 5′-flanking region was shown to enhance the promoter activity [35], and the GC-box (−267/−259) and CRE (−697/−690) located in these two domains are potential candidates for promoting the hCGT transcription because they have also been shown to regulate the expression of a number of myelin-specific genes [37]. To investigate whether these putative *cis*-acting elements and their cognate transcription factors are involved in the hCGT gene expression, the GC-box and CRE were further

characterized. In order to confirm the specificity of the two sequences in hCGT expression, we performed mutagenesis on the GC-box and CRE in the luciferase reporter plasmids, and the corresponding promoter activities were determined upon transient transfection into HOG cells. In assessing the proximal region of −292/−256, the 37-bp regulatory sequence that contains the GC-box (−267 TGGGCGGGG −259) is a potential candidate to explain the regulation of hCGT transcription. Two mutant reporter constructs containing disrupted GC-box were prepared: phCGT(mutated GC)Luc, containing a specific base change at position −263 (changing the consensus GC-box to TGGGAGGGG), and phCGT(deleted GC)Luc which is missing 7 bp (GGGCGGGG) of the GC-box sequence (Figure 2A). After transient transfection into HOG cells, the transcription activity conferred by these mutant GC-box constructs was significantly lower than that conferred by phCGT(−332)Luc construct ($P < 0.05$), validating the crucial regulatory role of this GC-box (Figure 2B).

Within the 60-bp distal regulatory sequence (from −747 to −688), the CRE site (−697 ATTCGTCA −670) is a potential candidate for cell-specific regulation of hCGT. To determine if this CRE sequence is crucial for the transcription of hCGT gene, we created the mutant construct, phCGT(deleted CRE)Luc which did not contain the CRE site (Figure 3A). As shown in Figure 3B, the promoter activity obtained from phCGT(deleted CRE)Luc was significantly reduced to less than half of that seen with the wild-type construct, phCGT(−717)Luc ($P < 0.05$), suggesting that this CRE motif is essential for enhanced hCGT transcription.

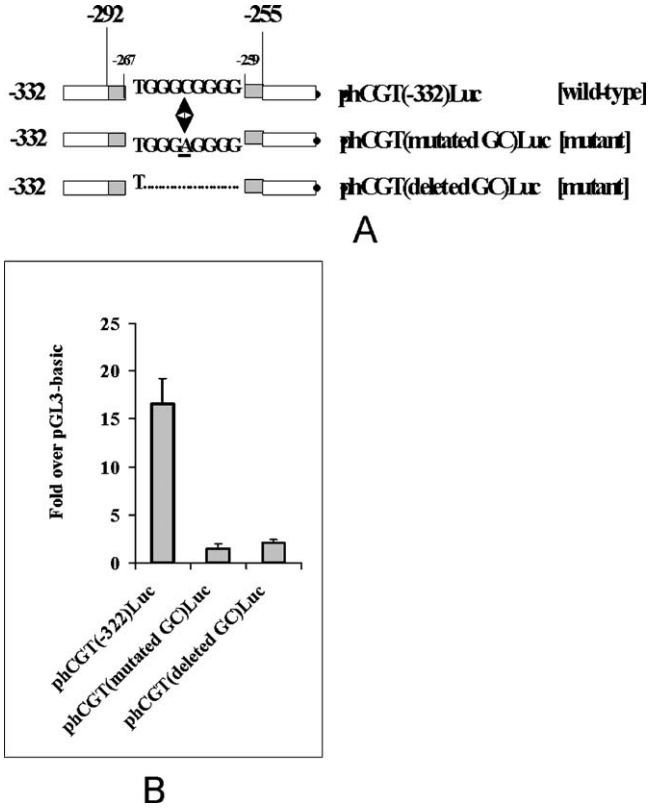

Figure 2. Mutation analysis of the GC-box (−267 TGGGGCGGGG −259) within the hCGT proximal *cis*-region . (A) A schematic representation of the hCGT proximal promoter constructs which contain either functional or disrupted GC-box inserted upstream of the luciferase coding region (indicated as a black arrow) in the pGL3-basic vector. The mutant reporter constructs were generated using either point mutation (C→A) or 7-bp deletion as indicated. Location of the positive regulatory region is included in the two gray boxes. The recognition site for the GC-box is indicated by the sense strand of DNA only. The sequence of deleted nucleotides is represented by a dotted line. (B) Functional activity of these reporter constructs in HOG cells. The luciferase activities of each deletion construct were normalized to the β-galactosidase activities. Activities are expressed as fold induction over pGL3-basic vector. Each value represents the mean ± S.D. of at least three independent sets of transfection experiments. Each set was performed in triplicate.

Analysis of the specific interactions between the putative transcriptional elements and nuclear proteins

Having determined that both GC-box and CRE motifs were necessary for high promoter activity in HOG cells, we then investigated the interaction of these regulatory elements with nuclear proteins. We utilized nuclear extracts from both HOG and LAN-5 cells since we expected to determine if the cell-specific expression of the hCGT gene was controlled by any of these transcriptional elements. Two double-stranded synthetic oligonucleotides spanning either of these regulatory regions were analyzed by EMSA to compare the *trans*-acting factors from the two cell lines.

Using radiolabeled "native GC" probe, a simple EMSA pattern was displayed (Figure 4). The left and right *panels* show the EMSA results were run in the same gel in order to compare the mobility and intensity of each complex between the two nuclear extracts. The same three protein-DNA complexes were present in nuclear extracts from both cell lines (*lane* 1), indicating that the corresponding EMSA complexes were formed with equivalent nuclear proteins and similar affinity. Our competition experiments indicated that all three protein-DNA complexes were sequence-specific, since the presence of a 50-fold molar excess of the unlabeled "native GC" probe competed out the complex formation (*lane* 2). Consistently, the presence of a 50-fold molar excess of unlabeled "consensus GC" probe was also able to compete with these EMSA complexes (*lane* 3), whereas competition was not observed using a 50-fold molar excess of unlabeled "mutated GC" probe which did not alter the complex formation (*lane* 4). The identity of these EMSA complexes was identified by adding antibodies against specific transcription factors to the binding reaction. The GC-box binding proteins included at least four distinct but closely related transcription factors, Sp1-Sp4 [39,40]. Therefore, we performed EMSA using two polyclonal antibodies, anti-Sp1 and anti-Sp3. As verified by

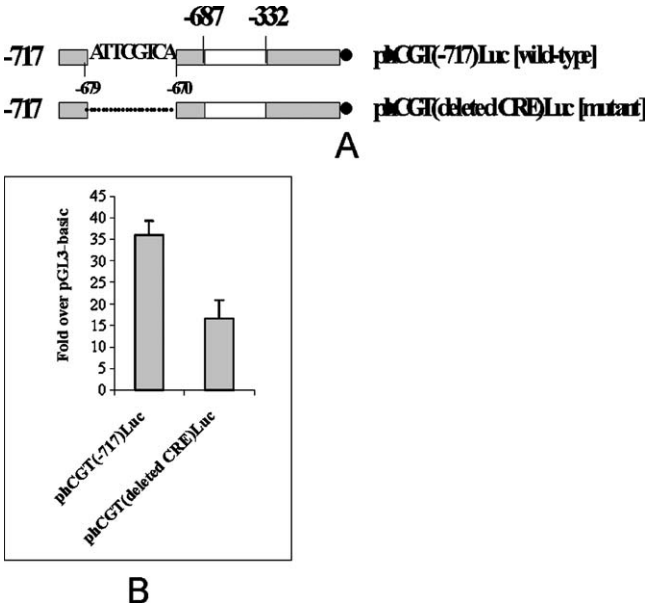

Figure 3. Mutation analysis of the CRE motif (−697 ATTCGTCA −690) within the hCGT distal *cis*-region. (A) A schematic representation of the hCGT distal promoter constructs which contain either functional or deleted CRE motif inserted upstream of the luciferase coding region (indicated as a black arrow) in the pGL3-basic vector. Locations of the positive regulatory regions are indicated within the gray boxes. The recognition site for CRE is indicated by the sense strand of DNA sequence only. The sequence of deleted nucleotides is represented by a dotted line. (B) Functional activities of these reporter constructs in HOG cells. The luciferase activities of each deletion construct were normalized to the β-galactosidase activities. Activities are expressed as fold induction over pGL3-basic vector. Each value represents the mean ± S.D. of at least three independent sets of transfection experiments. Each set was performed in triplicate.

quantitating the EMSA complexes, anti-Sp1 antibody caused the super-shift of the slowest and moderate DNA-protein complexes to a position of lower mobility (*lanes* 5 and 6); whereas, the addition of anti-Sp3 antibody resulted in the super-shift of the moderate and fastest migrating complexes, corresponding to their different isoforms (*lanes* 7 and 8) [41–43]. Thus, this EMSA profile revealed the binding pattern, consistent with the previous finding that Sp1 and Sp3 proteins were major components of these DNA-protein complexes [41,42].

In EMSA using the labeled "native CRE" probe, a different binding profile was observed: two complexes (I and II) were detected with the HOG nuclear extract (Figure 5, *lane* 1 of left *panel*), but only one complex (I) was detected with the LAN-5 nuclear extract (Figure 5, *lane* 1 of right *panel*). Although complex I was common between the two cell lines, differences in band intensity and degree of competition were noticed. Complex I formed was more intense using nuclear extracts from LAN-5 cells than HOG cells (*lane* 1). However, it was easier to compete out this complex using unlabeled competitors in LAN-5 than HOG nuclear extract (*lanes* 2 and 3). Our competition experiments demonstrated that the protein-DNA complexes shown in both panels were sequence-specific, since the presence of a 50-fold molar excess of the unlabeled "native CRE" probe and unlabeled "consensus CRE" probe was able to compete with these EMSA complexes (*lanes* 2 and 3, respectively). However, a slight competition was also observed using a 50-fold molar excess of unlabeled "mutated CRE" probe (*lane* 4). Since there are multiple members in the ATF/CREB transcription factor family [44], we wanted to determine whether the transcription factors in this family were truly involved in the EMSA complexes. It was unclear from supershift assays using CREB-1 monoclonal antibody since we only observed the slight reduction of DNA-protein complexes without obvious supershifted bands (data not shown). However, we clearly observed three supershifted bands (shown by *arrow heads*) using pCREB-1 polyclonal antibody in nuclear extracts from both cell types (*lane* 5). The ATF-1 monoclonal antibody also caused the formation of two noticeable supershifted bands at the similar positions as the supershifts generated by pCREB-1 antibody in both nuclear extracts (*lane* 6). Furthermore, the intensities of the DNA-protein complexes were dramatically reduced upon incubation with either pCREB-1 or ATF-1 antibodies. Although a similar supershifted profile was observed using nuclear extracts from both cell types, the supershifted bands produced were more intense in HOG cells than LAN-5 cells as confirmed by quantitating the band intensities.

The nuclear levels of Sp1, Sp3, CREB-1, pCREB-1, and ATF-1 proteins in HOG and LAN-5 cells

Since we found that GC-box and CRE sequences were important for the transcriptional activity of hCGT promoter in HOG cells to a much higher degree than in LAN-5 cells, the differential transactivation may be contributed to the difference in expression levels of their cognate transcription factors. To test this possibility, we determined the levels of Sp1, Sp3, CREB-1, pCREB-1, and ATF-1 in nuclear extracts from both cell types using Western blot analysis, employing specific antibodies (see "Materials and methods"). We found that the levels of Sp1 and Sp3 in the nucleus of HOG and LAN-5 cells were comparable (data not shown), suggesting that the differential promoter activity between the two cell types is unlikely due to the levels of these transcription factors in the nucleus. To determine the expression levels of the transcription factors in the ATF/CREB family, we first probed the blot with a polyclonal antibody specific for CREB-1, and we observed that CREB-1 was expressed in both cell lines in a comparable level as shown in Figure 6. Next, we probed the blot with a peptide-directed polyclonal antibody against pCREB-1. This antibody also recognizes phosphorylated forms of other ATF/CREB family members, including ATF-1 and CREM. Two bands with different intensities were seen in HOG and LAN-5 cells. The protein corresponding to the slower migrating band equivalently expressed in both cell types was a molecular size of approximately 43 kDa, suggesting it may correspond to CREB-1.

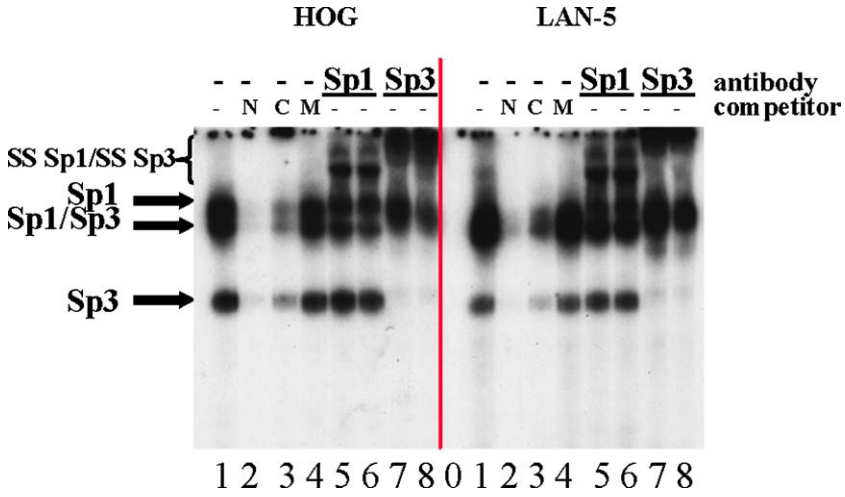

Figure 4. Detection of nuclear proteins from HOG and LAN-5 cells that bind to the GC-box (−267/−259) by EMSA. The experiments were performed using 5 μg of nuclear extracts, prepared from either HOG (left *panel*) or LAN-5 (right *panel*) cells, and radiolabeled "native GC" probe (N). The reaction without any nuclear extract added was also included to serve as a negative control (*lane* 0). Incubations were conducted in the absence (*lanes* 0, 1, 5–8) or presence [*lane* 2, native GC; *lane* 3, consensus GC (C); *lane* 4, mutated GC (M)] of 50-fold molar excess of unlabeled competitors. Binding reactions were further analyzed by including either anti-Sp1 antibody (*lane* 5, 4 μg; *lane* 6, 8 μg) or anti-Sp3 (*lane* 7, 4 μg; *lane* 8, 8 μg). Arrows indicate positions of the specific bands of Sp1 and Sp3 proteins. The supershifted bands of Sp1 (SS Sp1) and Sp3 (SS Sp3) are also observed.

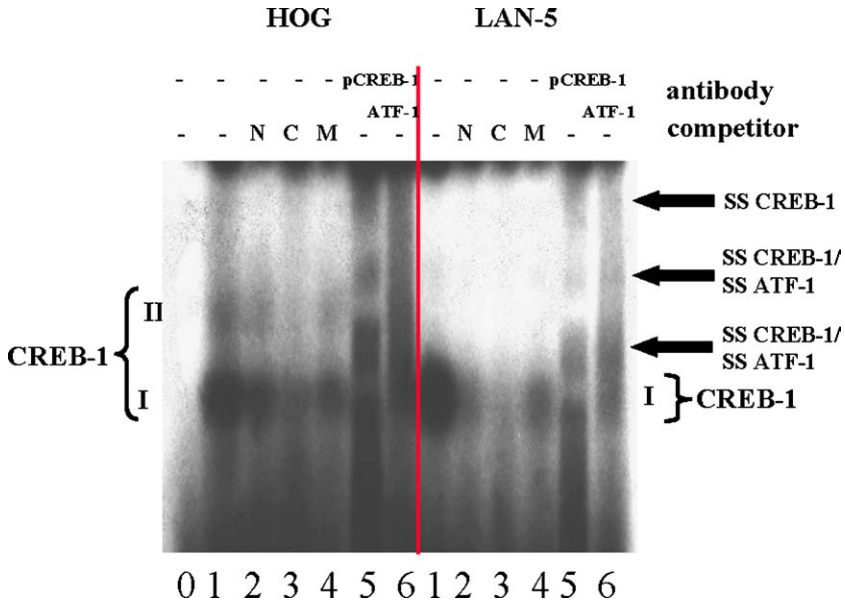

Figure 5. Detection of nuclear proteins from HOG and LAN-5 cells that bind to the CRE motif (−697/−690) by EMSA. The experiments were performed using 5 μg of nuclear extracts (*lanes* 1–6), prepared from either HOG (left *panel*) or LAN-5 (right *panel*) cells, and radiolabeled "native CRE" probe (N). The reaction without any nuclear extract added was also included to serve as a negative control (*lane* 0). Incubations were conducted in the absence (*lanes* 0, 1, 5, and 6) or presence [*lane* 2, native CRE; *lane* 3, consensus CRE (C); *lane* 4, mutated CRE (M)] of 50-fold molar excess of unlabeled competitors. Binding reactions were further analyzed by including either anti-pCREB-1 antibody (*lane* 5, 8 μg) or anti-ATF-1 antibody (*lane* 6, 8 μg). Arrows indicate positions of the specific bands of supershifted pCREB-1 (SS CREB-1) and ATF-1.

In contrast, the protein corresponding to the faster migrating band was expressed at much higher levels in HOG cells than in LAN-5 cells. The molecular size of the lower band suggested it might be ATF-1 which was confirmed by probing the blot with a monoclonal antibody specific for ATF-1. Thus, ATF-1 is clearly a strong candidate to explain the differential expression of hCGT transcripts between HOG and LAN-5 cells.

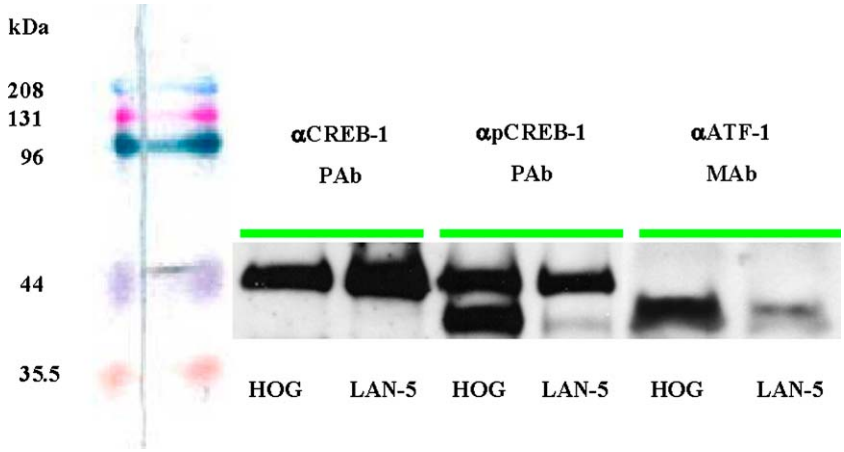

Figure 6. Expression of CREB-1, pCREB-1, and ATF-1 proteins in the nuclear extracts of HOG and LAN-5 cells. Twenty-five μg of nuclear extracts from either the HOG or the LAN-5 cells together with the molecular size makers were fractionated by SDS-polyacrylamide gel electrophoresis and electrotransferred to a nitrocellulose membrane. The blots were probed using either polyclonal (PAb) or monoclonal (MAb) antibodies as indicated. The specific proteins were detected using the chemiluminescence system. The positions of molecular size makers are shown on the left. Immunoblotting was performed using anti-CREB-1, anti-pCREB-1, and anti-ATF-1 antibodies.

Discussion

Recently, we reported the cloning and characterization of the hCGT gene promoter [35]. While the 5′-flanking regions of human [35] and mouse CGT [34] genes demonstrated significant sequence divergence, several putative transcriptional regulatory motifs were conserved. For instance, a GC-box motif was identified in the CGT promoters of both mouse and human genes. In addition, putative binding sites for cAMP-dependent transcription factors were also identified in the 5′-flanking regions of these genes; the binding site for suppressed-cAMP-inducible-protein (SCIP) was found in the mouse CGT gene, while that for CREB was identified in the human gene. A notable difference between the two promoters is the absence of myelin transcription factor 1 (MyT1) and Krox20/24 in the hCGT gene-promoter. These two regulatory elements have been shown to be unique and specific to myelinating glia [37,45]; however, it is not known to date whether their presence in the mouse CGT promoter contributes to the promoter activity. In the present study, we have further identified and characterized *cis*-elements and cognate *trans*-acting factors that regulate the expression of the hCGT gene.

Since the region located between the proximal and distal promoter regions of the hCGT gene is also essential for the high promoter activity, this distance-dependent characteristic may be responsible for the cooperative interactions between transcription factors bound to both positive proximal and distal regions. These protein-protein interactions are commonly known to be mediated by transcription factors bound to different regulatory regions of the gene, and the optimal distance between these regions is responsible for providing appropriate contacts. The deletion of the proximal region, while the distal region is still intact, eliminates the hCGT promoter activity. This result indicates that the distal regulatory region is functionally dependent on the proximal promoter region, which also implicates that the presence of the proximal core promoter is definitively required for transcription initiation.

The proximal (−292/−256) and distal (−747/−688) positive domains of hCGT gene are of particular interest because they contain the potential transcriptional elements, GC-box and CRE, respectively, and because they are sufficient to induce promoter activity by about 33-fold over pGL3-basic vector in HOG cells. Our results were also consistent with evidence that these two elements have been shown to regulate the expression of a number of myelin-specific genes [37]. Thus, our current investigation points to the significance of these two *cis*-elements in regulating the hCGT gene transcription.

Firstly, we demonstrated that a consensus GC-box (−267 TGGGCGGGG −259), known to be recognized by the Sp family of transcription factors, was definitively required to promote the hCGT transcription in HOG cells, as confirmed by mutation analysis. This element may enhance transcription activity from a distance through DNA looping mediated by protein-protein interactions [46]. Sp1 has also been shown to be involved in the basal transcription complex of several myelin-specific genes, such as myelin-associated glycoprotein (MAG), MBP, protein zero (P_0), and peripheral myelin protein-22 (PMP-22) [37]. The promoter activity driven by this GC-box is unlikely to be cell type-specific, since the same construct promotes expression of the reporter gene in LAN-5 cells to some extent [35]. This assumption is consistent with the results of EMSA and Western blot analysis, which showed that there is no notable difference between the binding and expression patterns of the corresponding nuclear proteins from HOG and LAN-5 cells. Using antibodies against Sp1 and Sp3 proteins, we showed that these two proteins were components of the respective EMSA complexes

that have also been described previously [41–43]. Previous reports have documented that Sp1 and Sp3 can interact with each other to either synergize or antagonize each other's activity at any given DNA-binding site [47–49]. Sp1 has been primarily shown to act as a positive transactivating factor [42]. Sp3 exists in three isoforms, generated by different translation start sites [43], all of which can act, to varying degrees, as activators or repressors of transcription, depending on the type of cells cell and promoter context [41,42,47,48,50]. In particular, two internally initiated Sp3 proteins can bind to the GC-box and function as potent inhibitors of Sp1/Sp3 mediated transcription. Thus, Sp1, in combination with the one long and two short isoforms of Sp3, may exert positive or negative effects on the transactivation of the hCGT promoter, apparently by competing for the same *cis*-element. It should be noted that our finding is the first ever to report the potential involvement of Sp3 in myelin-specific gene regulation.

Secondly, in contrast to the GC-box, there is a significant difference in the CRE-dependent promoter activity between HOG and LAN-5 cells [35]. EMSA and mutation analysis further confirmed the vital role of the CRE motif (−697 ATTCGTCA −690). However, there was a difference in EMSA profiles between HOG and LAN-5 cells, which may account for the differential transcription of the hCGT gene in the two cell types. The EMSA competition assay also demonstrated the higher binding affinity between "native CRE" probe and nuclear proteins of HOG cells than with LAN-5 cells. Although pCREB-1 and ATF-1 were components of the EMSA complexes of nuclear extracts from both cell types, the supershifted bands formed were more intense in HOG cells than LAN-5 cells as measured quantitatively. Thus, the CRE motif has been shown not only to enhance the promoter activity in HOG cells, but also to contribute to the cell-specific expression of hCGT gene. The differential transcriptional activity of the hCGT gene may be due to the fact that the CRE motif is generally recognized by multiple ATF/CREB isoforms; some of these act as activators and others as repressors of transcription [44]. Since many transcription factors in the basic leucine zipper (bZIP) family bind to the CRE sequence as dimers [51], various combinations of homodimeric [52–54] or heterodimeric [53–59] forms with distinct binding specificities and transactivation abilities [60] can result in different levels of promoter activity. In conjunction with the difference in transcription activity and EMSA profile, we did detect the difference in nuclear levels of ATF-1 in the two cell lines as Western blot analysis revealed that the nuclear levels of ATF-1 is obviously higher in HOG cells than in LAN-5 cells. Therefore, ATF-1 is likely the major candidate at the present time to explain the difference in hCGT gene expression between HOG cells and LAN-5 cells. Further studies of the functional roles of ATF-1 involved in the hCGT transcription are being investigated.

The presence of this CRE site suggests that hCGT transcription is regulated by the cAMP second messenger pathway. An increase in CGT mRNA after 48 h of cAMP treatment and a 2-fold increase in the synthesis of GalC and SGalC have been observed in the N20.1 mouse oligodendroglial cell line [61]. cAMP analogues increase the synthesis of GalC in cultured oligodendrocytes [62], which is consistent with the studies of McMorris and co-workers [63–65]. Implication of cAMP in the expression of several myelin genes such as MBP, protein P_2 (P_2), P_0, proteolipid protein (PLP), MAG, myelin-oligodendrocyte glycoprotein (MOG), and PMP-22 has also been described [66–73]. Furthermore, substantial evidence for the involvement of CREB-1 in gene expression has been demonstrated in both oligodendrocytes [74–78] and Schwann cells [79–81].

In summary, this study has established the indispensable functional roles of the GC-box and CRE motifs in governing the hCGT gene expression. We have also shown that the CRE site is responsible for the cell-specific expression of the hCGT gene in HOG and LAN-5 cells. Further upstream sequences may play important roles in the enhancement of basal expression, but these regions of DNA have not been examined to date. Therefore, it will be important to identify additional essential regulatory elements, possibly further than −2.3 kb upstream from the transcription start site in order to determine the exact regulatory mechanisms of its cell-specific and developmental regulation in myelinating glia. Our investigation on the hCGT gene promoter regions along with identification of the potential transcription factors involved in this highly regulated and coordinated expression offers the opportunity for future studies in defining the transcriptional regulation of the hCGT gene at the molecular level.

Acknowledgments

The authors gratefully acknowledge the generous gift of the HOG cell line from Dr. Glyn Dawson and the LAN-5 cell line from Dr. Stephan Ladisch. We thank Dr. Stacey A. Kraemer for her critical comments on this manuscript, and Dr. Chalinee Ronpirin for her assistance with FluorChem™ Imaging System.

References

1 Morell P, Quarles H, Myelin formation, structure, and biochemistry, in *Basic Neurochemistry*, edited by Siegel GJ, Agranoff BW, Albers RW, Fisher SK, Uhler MD (Lippincott-Raven Publishers, Philadelphia, 1999), pp. 69–93.

2 Norton WT, Cammer W, Isolation and characterization of myelin, in *Myelin*, edited by Morell P (Plenum Press, New York, 1984), pp. 147–95.

3 Curatolo W, Glycolipid function, *Biochim Biophys Acta* **906**, 137–60 (1987).

4 Saito M, Yu RK, Glycolipids of the CNS, in *Molecular Biology of Multiple Sclerosis*, edited by Russell WC (Wiley-Liss, New York, 1997), pp. 219–29.

5 Fry, JM, Weissbarth S, Lehrer GM, Bornstein MB, Cerebroside antibody inhibits sulfatide synthesis and myelination and demyelinates in cord tissue cultures, *Science* **183**, 540–2 (1974).

6 Dorfman S, Fry J, Silberberg D, Antiserum induced myelination inhibition *in vitro* without complement, *Brain Res* **177**, 105–14 (1979).

7 Ranscht B, Wood PM, Bunge RP, Inhibition of *in vitro* peripheral myelin formation by monoclonal anti-galactocerebroside, *J Neurosci* **7**, 2936–47 (1987).

8 Dyer CA, Benjamins JA, Antibody to galactocerebroside alters organization of oligodendroglial membrane sheets in culture, *J Neurosci* **8**, 4307–18 (1988).

9 Dyer CA, Novel oligodendrocyte transmembrane signaling systems: Investigations utilizing antibodies as ligand, *Mol Neurobiol* **93**, 1–22 (1993).

10 Rosenbluth J, Liu Z, Guo D, Schiff R, Inhibition of CNS myelin development *in vivo* by implantation of anti-GalC hybridoma cells, *J Neurocytol* **23**, 699–707 (1994).

11 Stoffel W, Bosio A, Myelin glycolipids and their functions, *Curr Opin Neurobiol* **7**, 654–61 (1997).

12 Coetzee T, Suzuki K, Popko B, New perspectives on the function of myelin galactolipids, *Trend Neurosci* **21**, 126–30 (1998).

13 Dupree JL, Suzuki K, Popko B, Galactolipids in the formation and function of the myelin sheath, *Microsc Res Tech* **41**, 431–40 (1998).

14 Basu S, Schultz A, Basu M, Enzymatic synthesis of galactocerebroside from ceramide. *Fed Proc* **28**, 540 (1969).

15 Morell P, Radin NS, Synthesis of cerebroside by brain from uridine diphosphate galactose and ceramide containing hydroxy fatty acid, *Biochem* **8**, 506–12 (1969).

16 Basu S, Schultz A, Basu M, Roseman S, Enzymatic synthesis of galactocerebroside by a galactosyltransferase from embryonic chicken brain. *J Biol Chem* **243**, 4272 (1971).

17 Sato C, Yu RK, Myelin galactolipid synthesis in different strains of mice, *J Neurochem* **49**, 1069–74 (1987).

18 Sato C, Yu RK, Heterosis for brain cerebroside synthesis in mice, *Dev Neurosci* **12**, 153–8 (1990).

19 Sato C, Black JA, Yu RK, Subcellular distribution of UDP-galactose:ceramide galactosyltransferase in rat brain oligodendroglia, *J Neurochem* **50**, 1887–93 (1988).

20 Schulte S, Stoffel W, Ceramide UDPgalactosyltransferase from myelination rat brain: Purification, cloning and expression, *Proc Natl Acad Sci USA* **90**, 10265–9 (1993).

21 Stahl N, Jurevics H, Morell P, Suzuki K, Popko B, Isolation, characterization, and expression of cDNA clones that encode rat UDP-galactose:ceramide galactosyltransferase, *J Neurosci Res* **38**, 234–42 (1994).

22 Schaeren-Wiemers N, van der Bijl P, Schwab ME, The UDP-galactose:ceramide galactosyltransferase: Expression pattern in oligodendrocytes and Schwann cells during myelination and substrate preference for hydroxyceramide, *J Neurochem* **65**, 2267–78 (1995).

23 Bosio A, Binczek E, Stoffel W, Molecular cloning and characterization of the mouse CGT gene encoding UDP-galactose ceramide-galactosyltransferase (cerebroside synthetase), *Genomics* **35**, 223–6 (1996).

24 Bosio A, Binczek E, Le Beau MM, Fernald AA, Stoffel W, The human gene CGT encoding the UDP-galactose ceramide galactosyl transferase (cerebroside synthase): Cloning, characterization, and assignment to human chromosome 4, band q26, *Genomics* **34**, 69–75 (1996).

25 Coetzee T, Li X, Fujita N, Marcus J, Suzuki K, Francke U, Popko B, Molecular cloning, chromosomal mapping, and characterization of the mouse UDP-galactose:ceramide galactosyltransferase gene, *Genomics* **35**, 215–22 (1996).

26 Kapitonov D, Yu RK, Cloning, characterization, and expression of human ceramide galactosyltransferase cDNA, *Biochem Biophys Res Commun* **232**, 449–53 (1997).

27 Bosio A, Binczek E, Stoffel W, Functional breakdown of the lipid bilayer of the myelin membrane in central and peripheral nervous system by disrupted galactocerebroside synthesis, *Proc Natl Acad Sci USA* **93**, 13280–5 (1996).

28 Coetzee T, Fujita N, Dupree JL, Shi R, Blight A, Suzuki K, Popko B, Myelination in the absence of galactocerebroside and sulfatide: Normal structure with abnormal function and regional instability, *Cell* **86**, 209–19 (1996).

29 Coetzee T, Dupree JL, Popko B, Demyelination and altered expression of myelin-associated glycoprotein isoforms in the central nervous system of galactolipid-deficient mice, *J Neurosci Res* **54**, 613–22 (1998).

30 Bosio A, Binczek E, Haupt WF, Stoffel, W, Composition and biophysical properties of myelin lipid define the neurological defects in galactocerebroside- and sulfatide-deficient mice, *J Neurochem* **70**, 308–15 (1998).

31 Bosio A, Bussow H, Adam J, Stoffel W, Galactosphingolipids and axono-glial interaction in myelin of the central nervous system, *Cell Tissue Res* **292**, 199–210 (1998).

32 Dupree JL, Coetzee T, Blight A, Suzuki K, Popko B, Myelin galactolipids are essential for proper node of Ranvier formation in the CNS, *J Neurosci* **18**, 1642–9 (1998).

33 Marcus J, Dupree JL, Popko B, Effects of galactolipid elimination on oligodendrocyte development and myelination, *Glia* **30**, 319–28 (2000).

34 Popko B, Myelin galactolipids: Mediators of axon-glial interactions?, *Glia* **29**, 149–53 (2000).

35 Tencomnao T, Yu RK, Kapitonov D, Characterization of the human UDP-galactose:ceramide galactosyltransferase gene promoter, *Biochim Biophys Acta* **1517**, 416–23 (2001).

36 Yonemasu T, Nakahira K, Okumura S, Kagawa T, Espinosa de los Monteros A, de Vellis J, Ikenaka K, Proximal promoter region is sufficient to regulate tissue-specific expression of UDP-galactose: Ceramide galactosyltransferase gene, *J Neurosci Res* **52**, 757–65 (1998).

37 Wegner M, Transcriptional control in myelinating glia: Flavors and spices, *Glia* **31**, 1–14 (2000).

38 Celi FS, Zenilman ME, Shuldiner AR, A rapid and versatile method to synthesize internal standards for competitive PCR, *Nucleic Acids Res* **21**, 1047 (1993).

39 Dent CL, Smith MD, DS, The DNA mobility shift assay, in *Transcription Factors: A Practical Approach*, edited by Latchman DS (Oxford University Press, New York, 1999), pp. 1–25.

40 Bradford MM, A rapid and sensitive method for the quantitation of microgram quantities of protein utilizing the principle of protein-dye binding, *Anal Biochem* **72**, 248–54 (1976).

41 Lania L, Majello B, De Luca P, Transcriptional regulation by the Sp family proteins, *Int J Biochem Cell Biol* **29**, 1313–23 (1997).

42 Suske G, The Sp-family of transcription factors, *Gene* **238**, 291–300 (1999).

43 Kennett SB, Udvadia AJ, Horowitz JM, Sp3 encodes multiple proteins that differ in their capacity to stimulate or repress transcription, *Nucleic Acids Res* **25**, 3110–7 (1997).

44 Shaywitz AJ, Greenberg ME, CREB: A stimulus-induced transcription factor activated by a diverse array of extracellular signals, *Annu Rev Biochem* **68**, 821–61(1999).

45 Wegner M, Transcriptional control in myelinating glia: The basic recipe, *Glia* **29**, 118–23 (2000).

46 Fry CJ, Farnham PJ, Context-dependent transcriptional regulation, *J Biol Chem* **274**, 29583–6 (1999).

47 Hagen G, Muller S, Beato M, Suske G, Sp1-mediated transcriptional activation is repressed by Sp3, *EMBO J* **13**, 3843–51 (1994).

48 Kumar AP, Butler AP, Transcription factor Sp3 antagonizes activation of the ornithine decarboxylase promoter by Sp1, *Nucleic Acids Res* **25**, 2012–9 (1997).

49 Kwon HS, Kim MS, Edenberg HJ, Hur MW, Sp3 and Sp4 can repress transcription by competing with Sp1 for the core *cis*-elements on the human ADH5/FDH minimal promoter, *J Biol Chem* **274**, 20–8 (1999).

50 Yu JH, Schwartzbauer G, Kazlman A, Menon RK, Role of the Sp family of transcription factors in the ontogeny of growth hormone receptor gene expression, *J Biol Chem* **274**, 34327–36 (1999).

51 Yamamoto KK, Gonzalez GA, Biggs WH, Montminy MR, Phosphorylation-induced binding and transcriptional efficacy of nuclear factor CREB, *Nature* **334**, 494–8 (1988).

52 Hai TW, Liu F, Coukos WJ, Green MR, Transcription factor ATF cDNA clones: An extensive family of leucine zipper proteins able to selectively form DNA-binding heterodimers, *Genes Dev* **3**, 2083–90 (1989).

53 Foulkes NS, Borrelli E, Sassone-Corsi P, CREM gene: Use of alternative DNA-binding domains generates multiple antagonists of cAMP-induced transcription, *Cell* **64**, 739–49 (1991).

54 Laoide BM, Foulkes NS, Schlotter F, Sassone-Corsi P, The functional versatility of CREM is determined by its modular structure, *EMBO J* 12, 1179–91 (1993).

55 Hurst HC, Masson N, Jones NC, Lee KA, The cellular transcription factor CREB corresponds to activating transcription factor 47 (ATF-47) and forms complexes with a group of polypeptides related to ATF-43, *Mol Cell Biol* **10**, 6192–6203 (1990).

56 Hurst HC, Totty NF, Jones NC, Identification and functional characterization of the cellular activating transcription factor 43 (ATF-43) protein, *Nucleic Acids Res* **19**,4601–9 (1991).

57 Foulkes NS, Mellstrom B, Benusiglio E, Sassone-Corsi P, Developmental switch of CREM function during spermatogenesis: From antagonist to activator, *Nature* **355**, 80–4 (1992).

58 Kobayashi M, Kawakami K, ATF-1CREB heterodimer is involved in constitutive expression of the housekeeping Na, K-ATPase alpha 1 subunit gene, *Nucleic Acids Res* **23**, 2848–55 (1995).

59 Kvietikova I, Wenger RH, Marti HH, Gassmann M, The transcription factors ATF-1 and CREB-1 bind constitutively to the hypoxia-inducible factor-1 (HIF-1) DNA recognition site, *Nucleic Acids Res* **23**, 4542–50 (1995).

60 Benbrook DM, Jones NC, Different binding specificities and transactivation of variant CRE's by CREB complexes, *Nucleic Acids Res* **22**, 1463–9 (1994).

61 Studzinski DM, Ramaswamy R, Benjamins JA, Effects of cyclic AMP on expression of myelin genes in the N20.1 oligodendroglial cell line, *Neurochem Res* **23**, 435–41 (1998).

62 Pleasure D, Parris J, Stern J, Grinspan J, Kim SU, Incorporation of tritiated galactose into galactocerebroside by cultured rat oligodendrocytes: Effects of cyclic adenosine 3′,5′-monophosphate analogues, *J Neurochem* **46**, 300–2 (1986).

63 McMorris FA, Cyclic AMP induction of the myelin enzyme 2′,3′-cyclic nucleotide 3′-phosphohydrolase in rat oligodendrocytes, *J Neurochem* **41**, 506–15 (1983).

64 McMorris FA, Cyclic AMP induces oligodendroglial cerebroside and MBP, *Trans Am Soc Neurochem* **16**, 285 (1985).

65 Raible DW, McMorris FA, Oligodendrocyte differentiation and progenitor cell proliferation are independently regulated by cyclic AMP, *J Neurosci Res* **34**, 287–94 (1993).

66 Ye P, Kanoh M, Zhu W, Laszkiewicz I, Royland JE, Wiggins RC, Konat G, Cyclic AMP-induced upregulation of proteolipid protein and myelin associated glycoprotein gene expression in C6 cells, *J Neurosci Res* **31**, 578–83 (1992).

67 Ye P, Laszkiewicz I, Wiggins RC, Konat GW, Transcriptional regulation of myelin associated glycoprotein gene expression by cyclic AMP, *J Neurosci Res* **37**, 683–90 (1994).

68 Bharucha VA, Peden KW, Subach BR, Narayanan V, Tennekoon GI, Characterization of the *cis*-acting elements of the mouse myelin P2 promoter, *J Neurosci Res* **36**, 508–19 (1993).

69 Jensen NA, Smith GM, Garvey JS, Shine HD, Hood L, Cyclic AMP has a differentiative effect on an immortalized oligodendrocyte cell line, *J Neurosci Res* **35**, 288–96 (1993).

70 Anderson S, Miskimins R, Involvement of protein kinase C in cAMP regulation of myelin basic protein gene expression, *J Neurosci Res* **37**, 604–11 (1994).

71 Jaquet V, Pfend G, Tosic M, Matthieu JM, Analysis of *cis*-acting sequences from the myelin oligodendrocyte glycoprotein promoter, *J Neurochem* **73**, 120–8 (1999).

72 Saberan-Djoneidi D, Sanguedolce V, Assouline Z, Levy N, Passage E, Fontes M, Molecular dissection of the Schwann cell specific promoter of the PMP22 gene, *Gene* **248**, 223–31 (2000).

73 Afshari FS, Chu AK, Sato-Bigbee C, Effect of cyclic AMP on the expression of myelin basic protein species and myelin proteolipid protein in committed oligodendrocytes: Differential involvement of the transcription factor CREB, *J Neurosci Res* **66**, 37–45 (2001).

74 Sato-Bigbee C, Yu RK, Presence of cyclic AMP response element-binding protein in oligodendrocytes, *J Neurochem* **60**, 2106–10 (1993).

75 Sato-Bigbee C, Chan EL, Yu RK, Oligodendroglial cyclic AMP response element-binding protein: A member of the CREB family of transcription factors, *J Neurosci Res* **38**, 621–8 (1994).

76 Sato-Bigbee C, Pal S, Chu AK, Different neuroligands and signal transduction pathways stimulate CREB phosphorylation at specific developmental stages along oligodendrocyte differentiation, *J Neurochem* **72**, 139–47 (1999).

77 Sato-Bigbee C, DeVries GH, Treatment of oligodendrocytes with antisense deoxyoligonucleotide directed against CREB mRNA: Effect on the cyclic AMP-dependent induction of myelin basic protein expression, *J Neurosci Res* **46**, 98–107 (1996).

78 Johnson JR, Chu AK, Sato-Bigbee C, Possible role of CREB in the stimulation of oligodendrocyte precursor cell proliferation by neurotrophin-3, *J Neurochem* **74**, 1409–17 (2000).
79 Stewart HJ, Expression of c-Jun, Jun B, Jun D and cAMP response element binding protein by Schwann cells and their precursors *in vivo* and *in vitro*, *Eur J Neurosci* **7**, 1366–75 (1995).
80 Lee MM, Sato-Bigbee C, DeVries GH, Schwann cells stimulated by axolemma-enriched fractions express cyclic AMP responsive element binding protein, *J Neurosci Res* **46**, 204–10 (1996).
81 Yamada H, Suzuki K, Age-related differences in mouse Schwann cell response to cyclic AMP, *Brain Res* **719**, 187–93 (1996).